

Supporting Information for:

A Probe for the Detection of Hypoxic Cancer Cells

Shenzheng Luo ¹, Rongfeng Zou ², Junchen Wu ^{1,3*} and Markita P. Landry ^{3,4*}

¹Key Laboratory for Advanced Materials & Institute of Fine Chemicals, School of Chemistry and Molecular Engineering, East China University of Science and Technology Shanghai 200237, China.

²Division of Theoretical Chemistry and Biology, School of Biotechnology, KTH Royal Institute of Technology, SE-10691 Stockholm, Sweden.

³Department of Chemical and Biomolecular Engineering, University of California Berkeley, 476 Stanley Hall, Berkeley, California 94720, USA.

⁴California Institute for Quantitative Biosciences (qb3), University of California-Berkeley, Berkeley, CA 94720.

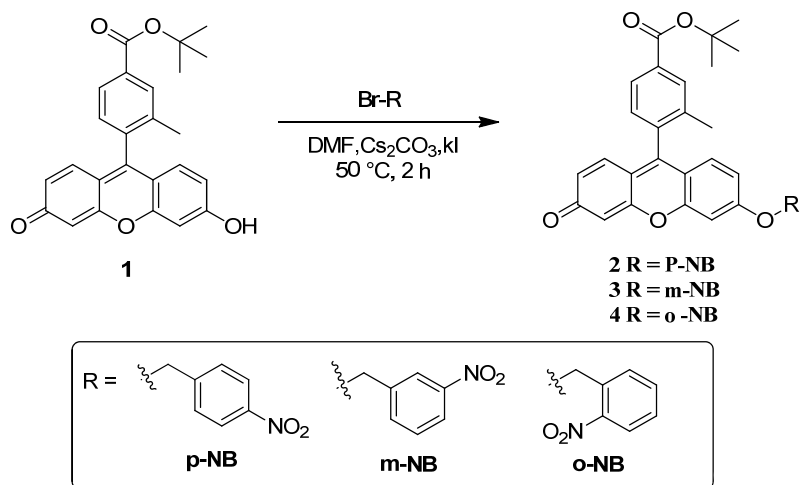
*E-mail: jcwu@ecust.edu.cn; landry@berkeley.edu

Table of contents

Synthesis route for intermediates of FBN-1–3.....	S3
Cell culture.....	S4
Cytotoxicity assay.....	S5
Fluorescence quantum yield determination.....	S5
HPLC analysis	S5
Detection limit	S6
Murine tumor model.....	S6
Figure S1. Calculated binding model of FBN-1.....	S7
Figure S2. The selectivity and kinetic curves of FBN-1 for NTR.....	S7
Figure S3. Fluorescence spectrum of FBN-1 response to NTR	S8
Figure S4. The fluorescence spectra of FBN-1 in the different reaction systems	S8
Figure S5. Mass spectrum of the reaction solution of FBN-1 with NTR	S9
Figure S6. HPLC profiles	S9
Figure S7. The structure and Molecular orbitals of FBN-1 and FD.....	S10

Figure S8. Cell photo-toxicity assay	S10
Figure S9. Cell viability assay	S11
Figure S10. Confocal fluorescence microscopy imaging	S11
Figure S11. Flow cytometry data	S12
Figure S12. Confocal fluorescence microscopy images of cells incubated with inhibitor	S12
Figure S13. Quantitative detection of NTR levels in cells by ELISA.....	S12
Figure S14. Quantitative detection of NTR levels in cells with inhibitor	S13
Figure S15. Quantification of the counts of figure 4a.....	S13
Figure S16. ¹ H NMR spectrum of compound 2.....	S14
Figure S17. ¹³ C NMR spectrum of compound 2.....	S14
Figure S18. Mass spectrum of compound 2.....	S15
Figure S19. ¹ H NMR spectrum of compound 3.....	S15
Figure S20. ¹³ C NMR spectrum of compound 3.....	S16
Figure S21. Mass spectrum of compound 3.....	S16
Figure S22. ¹ H NMR spectrum of compound 4.....	S17
Figure S23. ¹³ C NMR spectrum of compound 4.....	S17
Figure S24. Mass spectrum of compound 4.....	S18
Figure S25. ¹ H NMR spectrum of FBN-1.....	S18
Figure S26. ¹³ C NMR spectrum of FBN-1.....	S20
Figure S27. Mass spectrum of the FBN-1.....	S20
Figure S28. ¹ H NMR spectrum of FBN-2.....	S21
Figure S29. ¹³ C NMR spectrum of FBN-2.....	S21
Figure S30. Mass spectrum of the FBN-2.....	S22
Figure S31. ¹ H NMR spectrum of FBN-3.....	S22
Figure S32. ¹³ C NMR spectrum of FBN-3.....	S23
Figure S33. Mass spectrum of the FBN-3.....	S23

Synthesis route for intermediates of FBN-1–3



Scheme S1. Synthesis route of compound 2, 3 and 4.

Compound 1 1.0 g (2.5 mmol, 1 eq), Cs_2CO_3 1.7 g (5.0 mmol, 2 eq), and KI 0.4 g (2.5 mmol, 1 eq) in N, N-Dimethylformamide (20 mL) was heated to 50 °C, and then 8 mL of a DMF solution containing nitrobenzyl bromide (5.0 mmol, 2 eq) was added dropwise with stirring. The mixture was stirred for 2 h at 50 °C under an Ar atmosphere. The reaction was monitored with thin-layer chromatography. After the reaction was complete, the solvent was poured into dichloromethane (DCM; 50 mL) and the organic solution was washed with H_2O (80 mL \times 5), dried over anhydrous Na_2SO_4 , and filtered. The filtrate was added to silica gel and evaporated to dryness. The residue was purified on a silica gel column (DCM/MeOH = 450/1 \rightarrow 150/1) to generate the target compound.

Compound 2: 1.1 g (2.0 mmol, 81.8%, orange solid). ^1H NMR (400 MHz, CDCl_3) δ 8.29 (d, J = 8.7 Hz, 2H), 8.03 (s, 1H), 8.00 (d, J = 7.9 Hz, 1H), 7.64 (d, J = 8.7 Hz, 2H), 7.25 (d, J = 7.9 Hz, 1H), 7.03 (d, J = 2.4 Hz, 1H), 6.94 (d, J = 8.9 Hz, 1H), 6.88 (d, J = 9.7 Hz, 1H), 6.84 (dd, J = 8.9, 2.4 Hz, 1H), 6.56 (dd, J = 9.7, 1.9 Hz, 1H), 6.45 (d, J = 1.8 Hz, 1H), 5.30 (s, 2H), 2.13 (s, 3H), 1.65 (s, 9H); ^{13}C NMR (101 MHz, CDCl_3) δ 185.8, 165.1, 162.6, 158.6, 154.4, 148.0, 147.9, 142.8, 136.6, 136.5, 133.3, 131.5, 130.5, 130.1, 129.3, 129.2, 127.7, 127.2, 124.1, 118.5, 114.5, 113.8, 106.1, 101.6, 81.7, 69.3, 28.2, 19.6; FT-IR: ν [cm^{-1}] 3425, 3045, 2978, 2922, 1712, 1643, 1600, 1513, 1442, 1347, 1300, 1260, 1205, 1165, 1100, 1030, 905, 850, 764, 725, 600, 495; MS-ESI: m/z calculated for $\text{C}_{32}\text{H}_{27}\text{NO}_7$ $[\text{M}+\text{H}]^+$ 538.1866, found 538.1863; melting point: 223.1–224.5 °C.

Compound 3: 1.0 g (1.8 mmol, 74.3%, orange solid). ^1H NMR (400 MHz, CDCl_3) 8.34 (s, 1H), 8.24 (d, $J = 7.8$ Hz, 1H), 8.03 (s, 1H), 8.00 (d, $J = 7.9$ Hz, 1H), 7.79 (d, $J = 7.7$ Hz, 1H), 7.63 (t, $J = 7.9$ Hz, 1H), 7.25 (d, $J = 7.9$ Hz, 1H), 7.04 (d, $J = 2.4$ Hz, 1H), 6.95 (d, $J = 8.9$ Hz, 1H), 6.90 – 6.83 (m, 2H), 6.56 (dd, $J = 9.7, 1.9$ Hz, 1H), 6.46 (d, $J = 1.9$ Hz, 1H), 5.28 (s, 2H), 2.14 (s, 3H), 1.65 (s, 9H); ^{13}C NMR (CDCl_3) δ : 185.8, 165.1, 162.7, 158.6, 154.4, 148.6, 148.3, 147.9, 137.7, 136.6, 136.6, 133.3, 133.2, 131.5, 130.6, 130.2, 129.9, 129.3, 129.2, 127.2, 123.5, 122.2, 118.5, 114.5, 113.9, 106.1, 101.6, 81.7, 69.3, 28.2; FT-IR: ν [cm^{-1}] 3435, 2975, 2925, 2850, 1710, 1640, 1595, 1530, 1445, 1345, 1290, 1255, 1205, 1160, 1110, 1025, 905, 850, 765, 720, 670, 595, 495; MS-ESI: m/z calculated for $\text{C}_{32}\text{H}_{27}\text{NO}_7$ $[\text{M}+\text{H}]^+$ 538.1866, found 538.1871; melting point: 155.4–157.4 °C.

Compound 4: 0.8 mg (1.5 mmol, 60.0%, orange solid). The light was avoided during preparation. ^1H NMR (400 MHz, CDCl_3) δ 8.23 (d, $J = 8.2$ Hz, 1H), 8.03 (s, 1H), 8.00 (d, $J = 8.0$ Hz, 1H), 7.84 (d, $J = 7.8$ Hz, 1H), 7.73 (t, $J = 7.5$ Hz, 1H), 7.56 (t, $J = 7.7$ Hz, 1H), 7.24 (s, 1H), 7.06 (d, $J = 2.1$ Hz, 1H), 6.95 (d, $J = 8.9$ Hz, 1H), 6.92 – 6.84 (m, 2H), 6.57 (dd, $J = 9.7, 1.4$ Hz, 1H), 6.46 (d, $J = 1.4$ Hz, 1H), 5.62 (s, 2H), 2.14 (s, 3H), 1.65 (s, 9H); ^{13}C NMR (101 MHz, CDCl_3) δ 185.8, 165.1, 162.7, 158.6, 154.4, 147.9, 147.0, 136.6, 134.2, 133.3, 132.1, 131.5, 130.6, 130.1, 129.3, 129.2, 129.0, 128.5, 127.2, 125.3, 118.5, 114.5, 113.7, 106.2, 101.8, 81.7, 67.6, 29.7, 28.2, 19.6; FT-IR: ν [cm^{-1}] 3435, 2970, 2925, 2855, 1715, 1640, 1600, 1525, 1455, 1375, 1335, 1290, 1265, 1205, 1165, 1115, 1030, 910, 855, 730, 595, 500; MS-ESI: m/z calculated for $\text{C}_{32}\text{H}_{27}\text{NO}_7$ $[\text{M}+\text{H}]^+$ 538.1866, found 538.1866; melting point: 188.1–190.9 °C.

Cell Culture.

HepG-2, A549 and SKOV-3 cells (Bioleaf Biotech Co., Ltd.) were cultured in McCoy's 5A (Gibco), DMEM (Gibco) and RPMI-1640 (Gibco), respectively, at 37 °C under humidified conditions of 95% air and 5% CO_2 . All media were supplemented with 100 U penicillin, 10% fetal bovine serum and 0.1 mg of streptomycin (Gibco) per milliliter. The culture media were changed every 2 days to maintain exponential growth of the cells. Cells were passaged using 0.05% Trypsin/EDTA (Sigma) when they reached 80-90% confluence and seeded for experiments. For hypoxia condition experiments, the cells were incubated with FBN-1 (5 μM) for 30 min at 37 °C, and kept under normoxic (20% O_2) and hypoxic (15%, 8%, and 0.1% O_2) conditions for another 8 h, respectively.

Cytotoxicity Assay.

The cytotoxicity of FBN-1 to HepG-2, A549 and SKOV-3 cells was measured using standard MTT assays. Cells growing in log phase were seeded into 96-well cell-culture plates at 1×10^5 cells/well. The cells were incubated 24 h at 37 °C under humidified conditions of 95% air and 5% CO₂. Then, the three kinds of cells were treated with 1, 2, 4, 8, 16, 32 and 64 µM of FBN-1. Next, one set of plates was kept under dark conditions and MTT solution was added (10 µL, 5 mg/mL in PBS) for another 4 h incubation at 37 °C. The other set of plates were exposed to blue light (LED-light source with 490 nm filter, 0.25 W cm⁻²) for 30 min and subsequently incubated for an additional 30 min. After 1 h, the plates were taken out of the incubator, and the old medium was removed. Next, fresh medium was added, and the cells were allowed to recover for 4 h. Next, MTT solution (10 µL, 5 mg/mL in PBS) was added to the media for another 4 h incubation at 37 °C. Finally, cell culture media was removed from all plates prior to formazan extraction with 100 µL DMSO, which was subsequently analysed colorimetrically using a Multi-mode Plate Reader (BioTek, USA) at 570 nm (absorbance value). The following formula was used to calculate the viability of cell growth: Viability (%) = (mean absorbance value of the treatment group-blank/mean absorbance value of the control-blank) × 100.

Fluorescence Quantum Yield Determination.

Fluorescence quantum yields for the FBN-1 and FD were measured by a relative method using Fluorescein ($\Phi_F = 79\%$ in 0.1M NaOH, emission range: 500-600 nm) as a standard. The following equation was used to determine the relative fluorescence quantum yield:

$$\Phi_{F(X)} = \Phi_{F(S)} \times (I_{\text{sample}} / I_{\text{standard}}) \times (A_{\text{standard}} / A_{\text{sample}}) \times (n_{\text{sample}} / n_{\text{standard}})^2$$

Where Φ_F is the fluorescence quantum yield, A is the absorbance at the excitation wavelength (in the range of 0.02-0.05), I is the area under the emission curve, n is the refractive index of the solvents used in measurements.

HPLC analysis

Agilent SD-1 liquid chromatography (Agilent Technologies, Palo Alto, CA, USA) was performed with a RPC18 HPLC column (4.6×250 mm, 10 µm; Agilent Technologies) and UV detector. The

mobile phase was a gradient of 0-100% of acetonitrile aqueous solution containing 0.1% TFA at a total flow rate of 1 mL/min. The UV absorption wavelength at 254 nm was set for analysis.

Detection limit

The detection limit was calculated based on the fluorescence titration. The fluorescence enhancement of FBN-1 was dose-dependent with respect to NTR. The linear response ($y = 1920.1x + 59.4$ with $R = 0.992$) of fluorescent intensity (y) with respect to the concentration of NTR (x) was established. The lower detection limit (LDL) was calculated following equation. $LDL = 3S/m$ (S is the ratio signal and noise, which is the standard deviation of blank measurements, $n = 15$; m is the slope of linear equation).

Murine Tumor Model.

All animals were handled in accordance with our laboratory animal handling protocol, and conformed to the Guide for the Care and Use of Laboratory Animals. The HepG-2 cells were washed with PBS (pH 7.4) and harvested with 0.05% trypsin/EDTA (Sigma). After centrifugation, the harvested cells were suspended in PBS (pH 7.4). To create the tumor model, 6-week-old (approximately 20 g) female BALB/c nude mice were implanted subcutaneously on the right flank with 10^7 HepG-2 cells in 0.2 mL of PBS (pH 7.4). The tumors were allowed to develop for 7 or 35 days before the imaging and ELISA analyses.

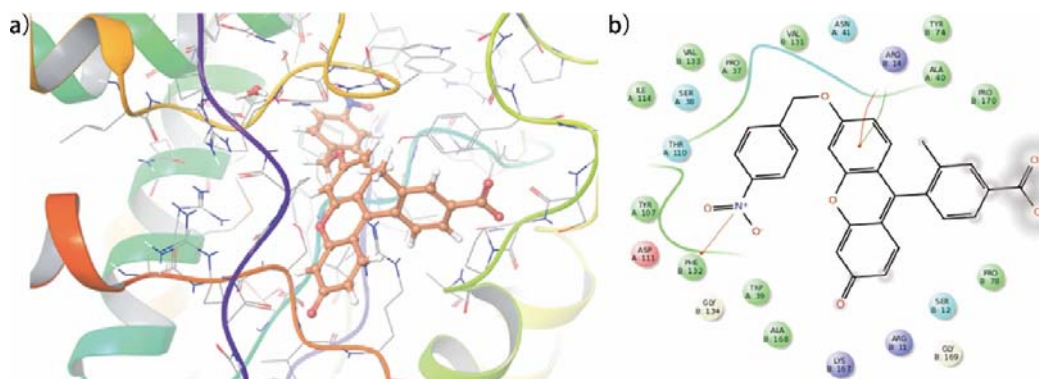


Figure S1. Calculated binding model of FBN-1. a) The substrate binding pocket of NTR (PDB ID: 4DN2) was generated using Schrödinger suites, the C, N, and O atoms of FBN-1 structure are shown in pink, blue, and red, respectively. b) The interactions between the best docking pose of FBN-1 and the active site amino acids of NTR active site in the best docked pose.

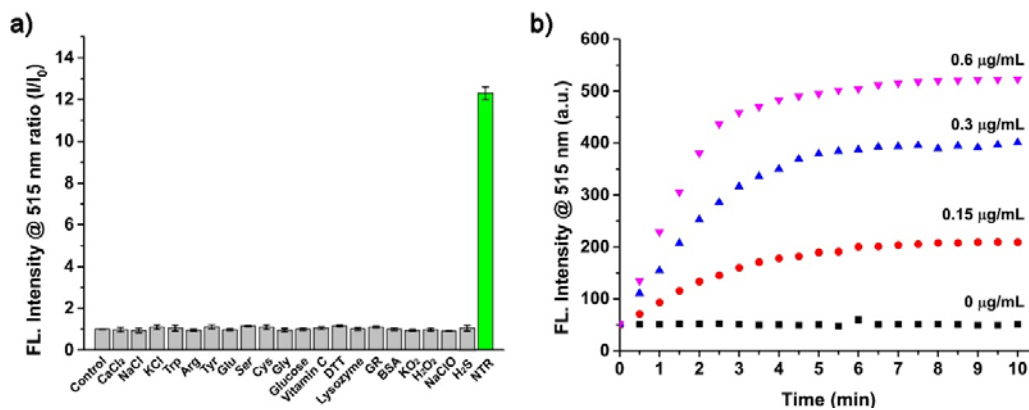


Figure S2. a) Fluorescence responses of FBN-1 (5 µM) to various species: control (FBN-1 + NADH) and with CaCl₂ (2.5 mM), NaCl (2.5 mM), KCl (50 mM), Trp (1 mM), Arg (1 mM), Tyr (1 mM), Glu (1 mM), Ser (1 mM), Cys (1 mM), Gly (1 mM), glucose (10 mM), vitamin C (1 mM), DTT (1 mM), lysozyme (0.5 mg/mL), GR (10 µg/mL), BSA (100 mg/mL), KO₂ (1 mM), H₂O₂ (1 mM), NaClO (1 mM), H₂S (1 mM) and NTR (0.6 µg/mL). b) Time-dependent fluorescence emission intensity of FBN-1 (5 µM) after reaction with different concentrations of NTR (0, 0.15, 0.3 or 0.6 µg/mL). $\lambda_{\text{ex}} = 490 \text{ nm}$.

As shown in **Figure S2**, the fluorescence intensity increases linearly for the first ~2 minutes of incubation of 5 µM FBN-1 with 0.6 µg/mL NTR, and subsides thereafter. Discrepancies in the final fluorescence intensity are attributed to different concentrations of DMSO used in each run, and associated sensitivities of NTR and NADH to such buffer conditions¹⁻³.

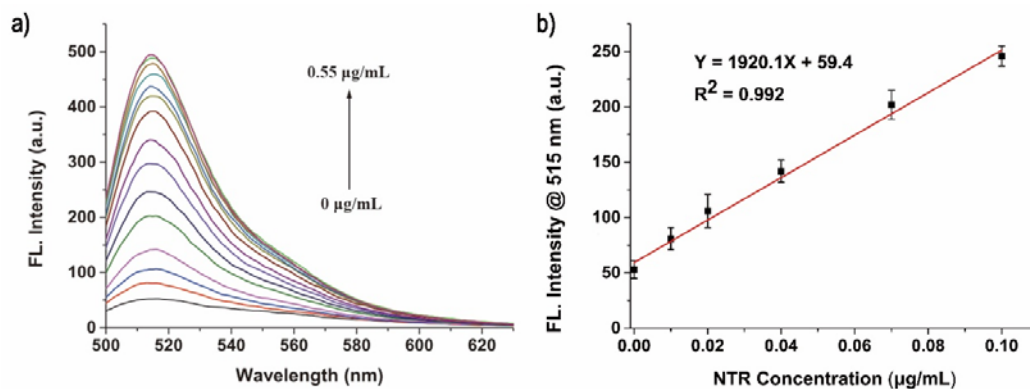


Figure S3. a) Fluorescence spectrum of FBN-1 (5 μM) response to NTR at varied concentrations (0, 0.01, 0.02, 0.04, 0.07, 0.1, 0.15, 0.2, 0.25, 0.3, 0.35, 0.4, 0.45, 0.5, 0.55 μg/mL). b) A linear correlation between emission intensity and concentrations of NTR. $\lambda_{\text{ex}} = 490$ nm.

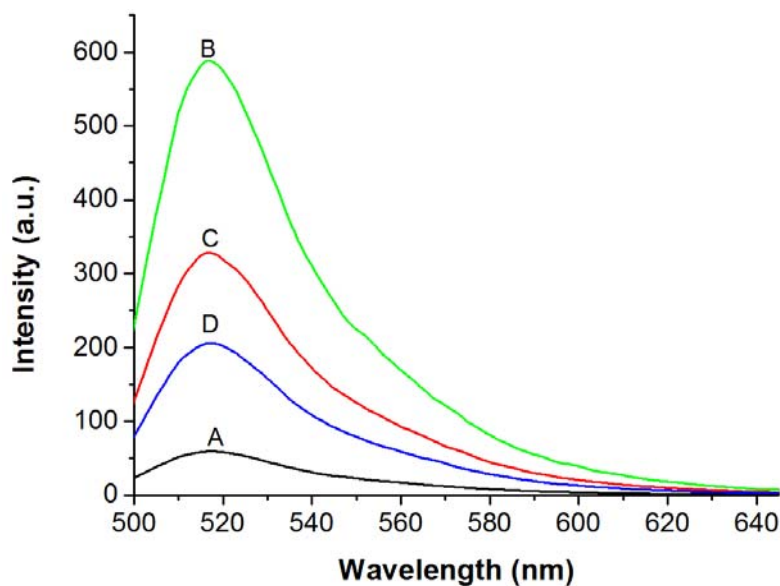


Figure S4. The fluorescence emission spectra of FBN-1 (5 μM) in the different reaction systems. (A): treated with 500 μM NADH and without NTR; (B): treated with 1 μg mL⁻¹ NTR and 500 μM NADH; (C): B system treated with 0.1 mM dicoumarin; (D): B system treated with 0.2 mM dicoumarin. $\lambda_{\text{ex}} = 490$ nm.

Elemental Composition Report

Single Mass Analysis

Tolerance = 500.0 PPM / DBE: min = -1.5, max = 100.0

Element prediction: Off

Number of isotope peaks used for i-FIT = 3

Monoisotopic Mass, Even Electron Ions

4 formula(e) evaluated with 1 results within limits (up to 1 best isotopic matches for each mass)

Elements Used:

C: 0-21 H: 0-15 O: 0-5

JC-WU

ECUST Institute of Fine Chem

JC-LSZ-1 9 (0.202) Cm (8:13)

Page 1

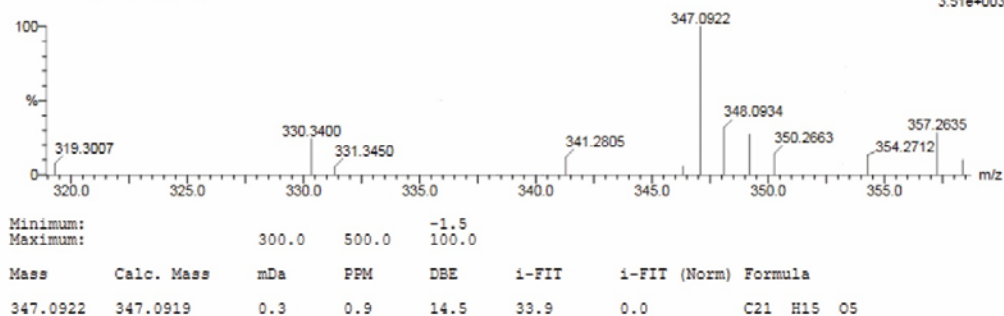
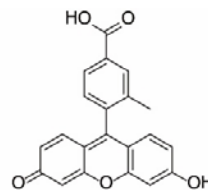


Figure S5. Mass spectrum of the reaction solution of FBN-1 (200 μ M) with NTR (20 μ g/mL).

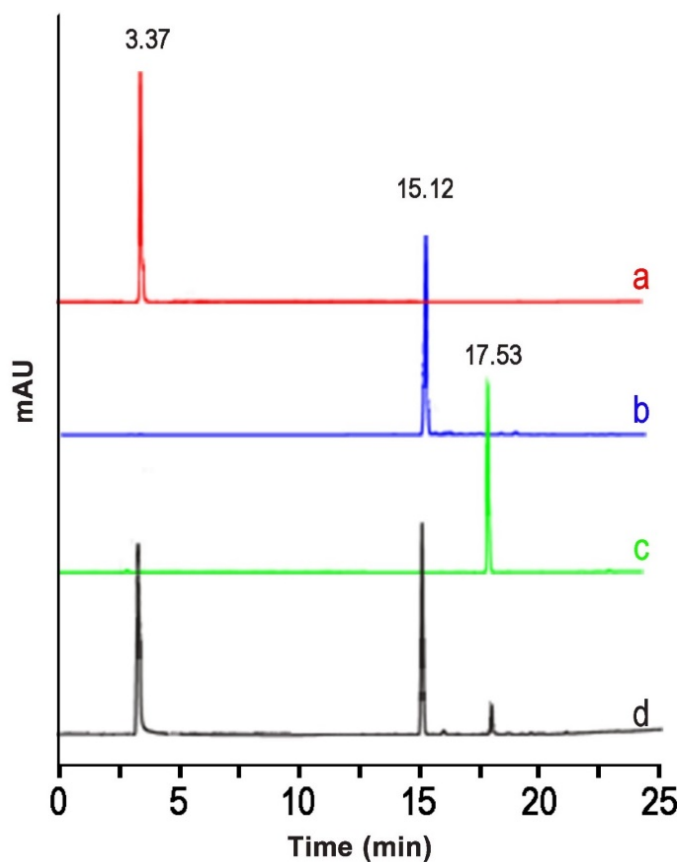


Figure S6. HPLC profiles of (a) 2 mM NADH, (b) 200 μ M fluorescein analogues, (c) 200 μ M FBN-1, (d) 200 μ M FBN-1 mixed with 20 μ g/mL NTR in the presence of 2 mM NADH for 20 min.

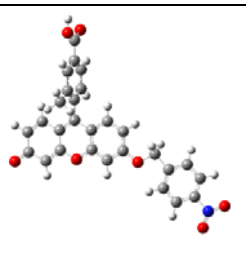
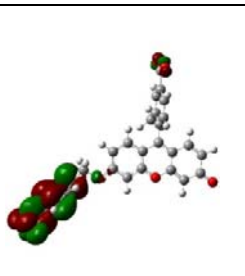
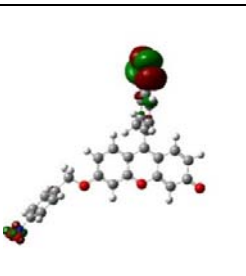
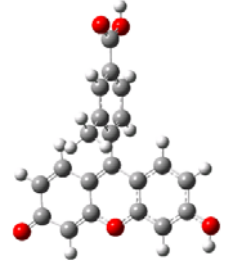
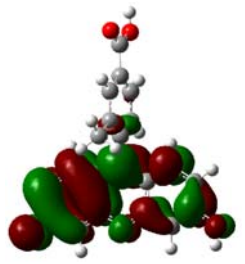
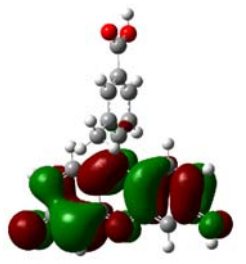
chemical structure	optimized structure	molecular orbitals	
		Lumo	Homo
			
			

Figure S7. The chemical structure, DFT optimized structure and Molecular orbitals (LUMO and HOMO) of FBN-1 and FD, respectively.

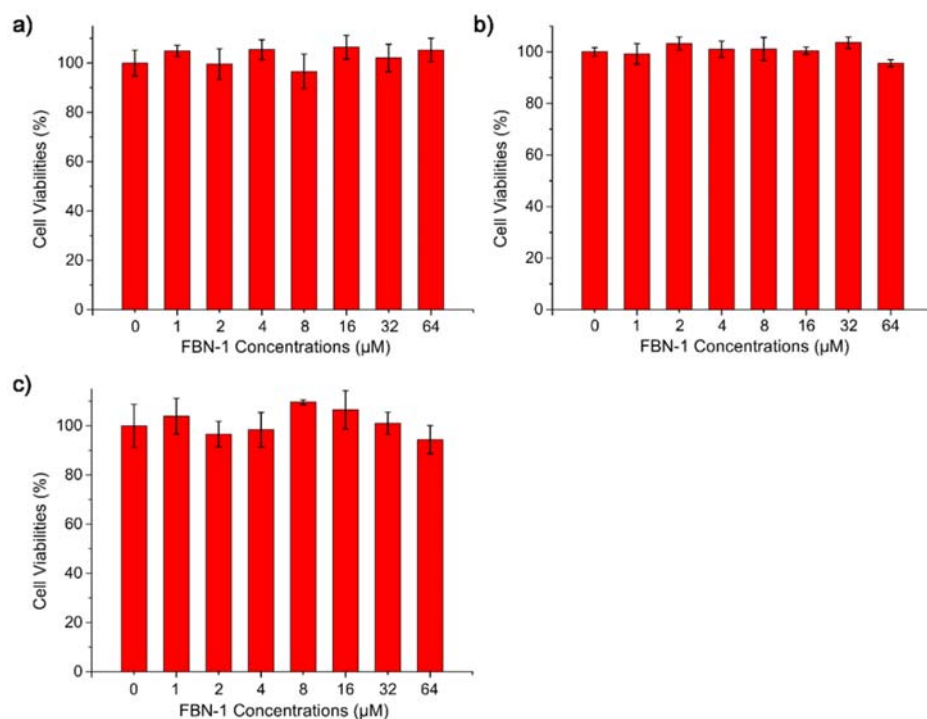


Figure S8. Cell viability (%) estimated by an MTT assay in a) HepG-2 cells, b) A549 cells, and c) SKOV-3 cells. Cells were treated with different concentrations of FBN-1 under blue light irradiation (490 nm, 0.25 W cm^{-2} , 30 min).

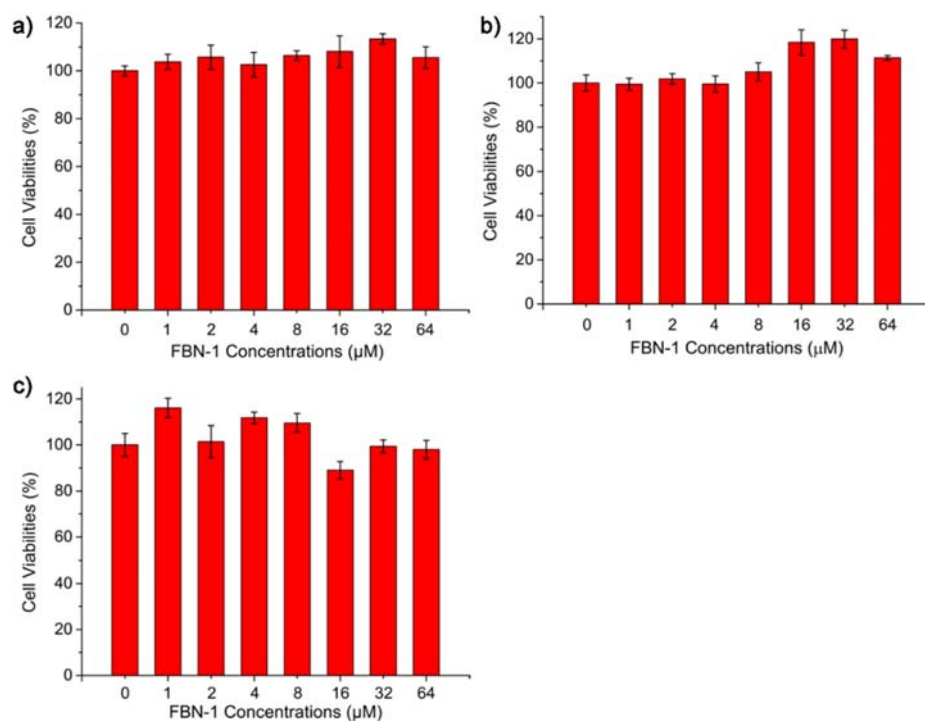


Figure S9. Cell viability (%) estimated by an MTT assay in a) HepG-2 cells, b) A549 cells, and c) SKOV-3 cells. Cells were treated with different concentrations of FBN-1 in the absence of blue light irradiation.

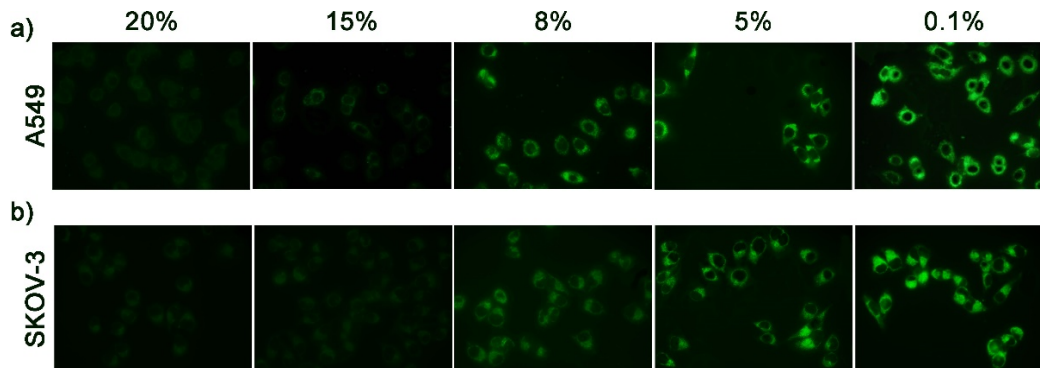


Figure S10. Confocal fluorescence microscopy imaging of a) A549 and b) SKOV-3 cells. A549 and SKOV-3 cells were incubated with FBN-1 (5 μM) under 20% O_2 , 15% O_2 , 8% O_2 , 5 % O_2 and 0.1 % O_2 conditions for 8 h.

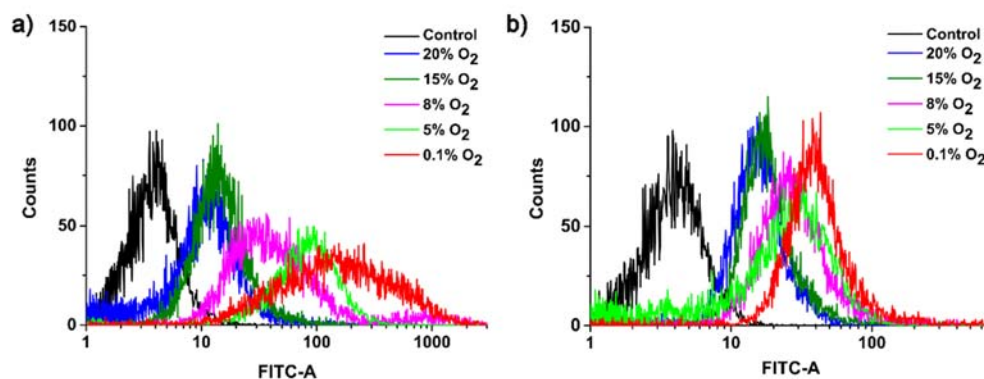


Figure S11. Flow cytometry of a) A549 and b) SKOV-3 cells. A549 and SKOV-3 cells were incubated with FBN-1 (5 μ M) under 20% O₂, 15% O₂, 8% O₂, 5 % O₂ and 0.1 % O₂ conditions for 8 h.

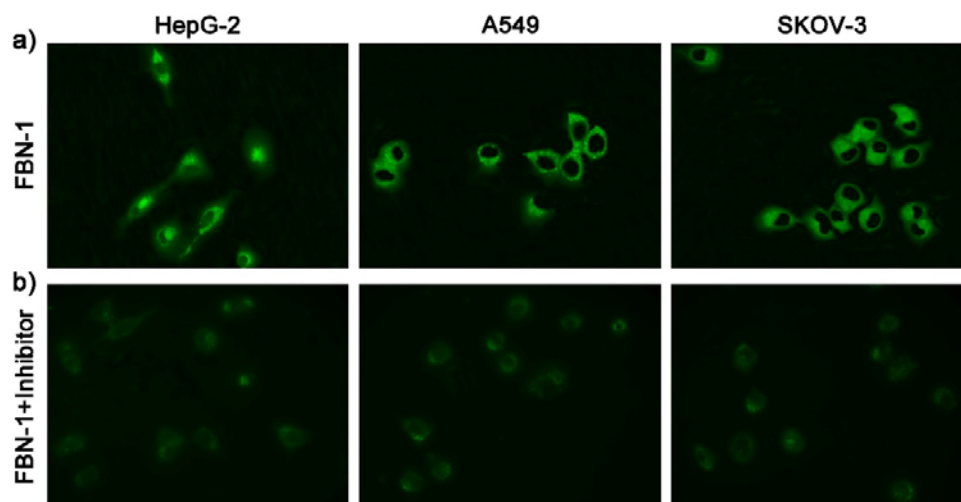


Figure S12. Confocal fluorescence microscopy imaging of HepG-2, A549 and SKOV-3 cells incubated with a) 5 μ M FBN-1 and b) 5 μ M FBN-1 and inhibitor (0.2 mM dicoumarin) under hypoxic condition of 1% O₂ for 8 h.

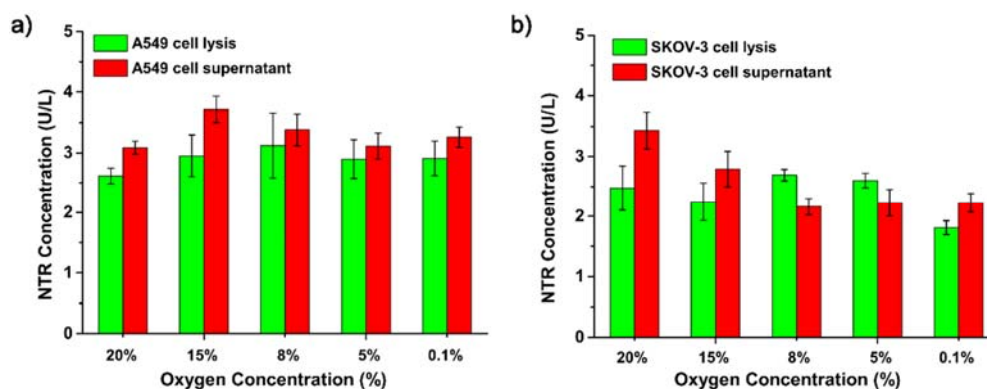


Figure S13. ELISA-based quantification of NTR concentration in a) A549 and b) SKOV-3 cell lysates and supernatant. A549 and SKOV-3 cells were incubated with FBN-1 (5 μ M) under 20% O₂, 15% O₂, 8% O₂, 5 % O₂ and 0.1 % O₂ conditions for 8 h.

Prior findings have claimed that NTR overexpression is likely linked to intensification of hypoxia. However, the reduction process of common NTR probes can be influenced by oxygen and nitroreductase as we show in **Scheme 2**. Our work in direct ELISA quantification of NTR in tumor cell lines, and in excised tumors, both suggest that NTR expression is invariant with degree of hypoxia, an effect which as not probed in prior work⁴⁻⁹.

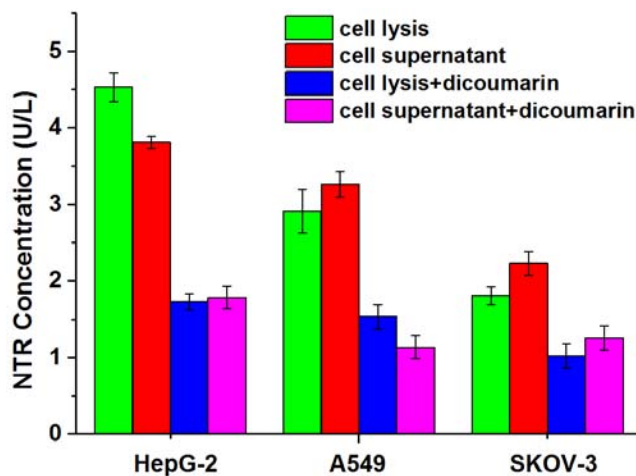


Figure S14. Quantitative detection of NTR levels in cell lysates, cell supernatant, cell lysates with 0.2 mM dicoumarin and cell supernatant with 0.2 mM dicoumarin by ELISA. HepG-2, A549 and SKOV-3 cells were incubated under 0.1 % O₂ conditions for 8 h at 37 °C.

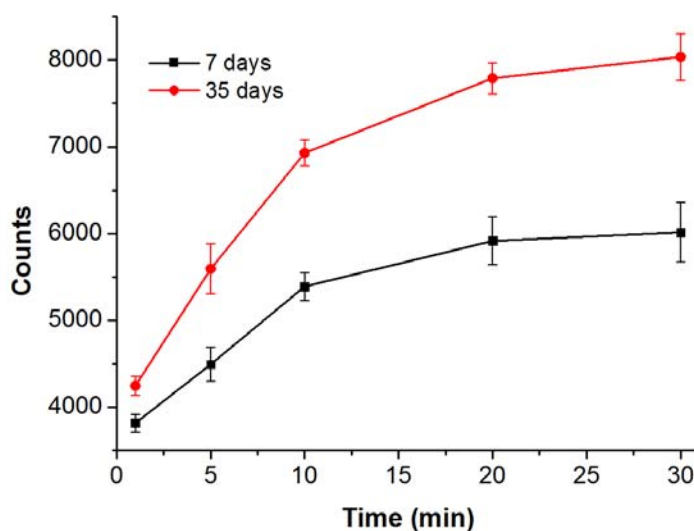


Figure S15. Quantification of the counts of figure 3a.

¹H NMR, ¹³H NMR and Mass Spectra

Compound 2:

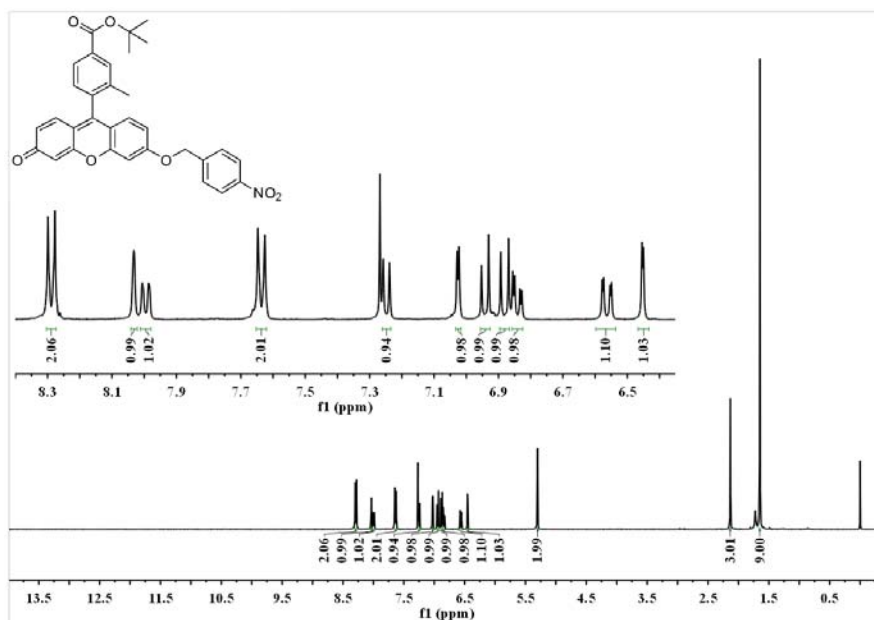


Figure S16. ¹H NMR spectrum of compound 2.

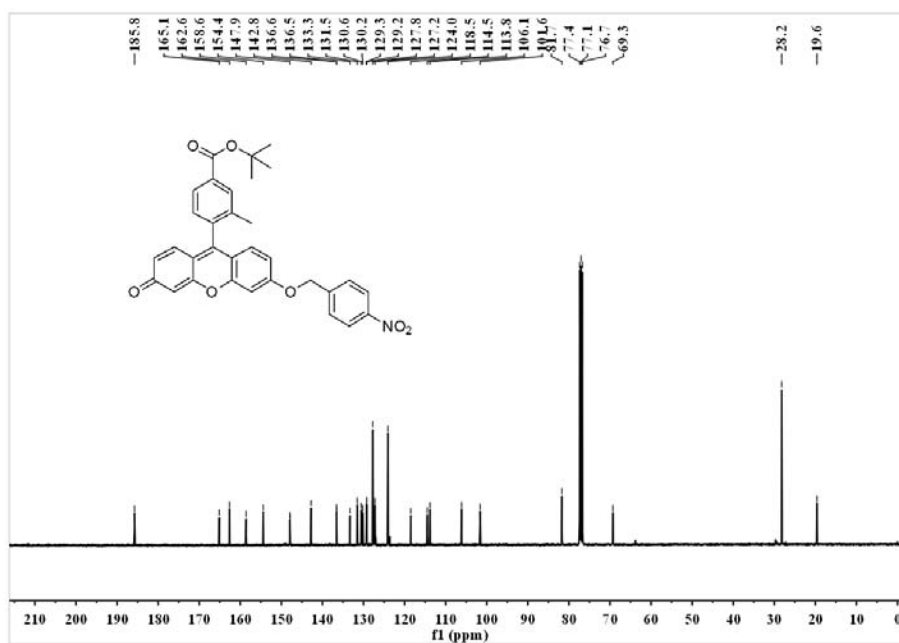


Figure S17. ¹³C NMR spectrum of compound 2.

Elemental Composition Report

Page 1

Single Mass Analysis

Tolerance = 50.0 PPM / DBE: min = -1.5, max = 100.0

Element prediction: Off

Number of isotope peaks used for i-FIT = 3

Monoisotopic Mass, Even Electron Ions

191 formula(e) evaluated with 13 results within limits (up to 1 closest results for each mass)

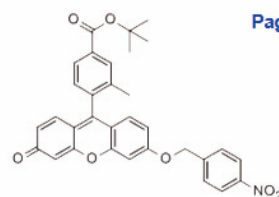
Elements Used:

C: 0-49 H: 0-49 N: 0-3 O: 0-10

JC-WU

ECUST institute of Fine Chem

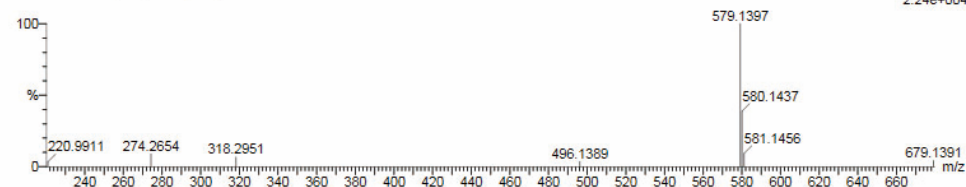
JC-LSZ-311 12 (0.168) Cm (11:28)



02-Jun-2016

20:11:39

1: TOF MS ES+
2.24e+004



Minimum: -1.5
Maximum: 300.0 50.0 100.0

Mass	Calc. Mass	mDa	PPM	DBE	i-FIT	i-FIT (Norm)	Formula
579.1397	579.1404	-0.7	-1.2	22.5	10.6	0.0	C32 H23 N2 O9

Figure S18. Mass spectrum of compound 2.

Compound 3:

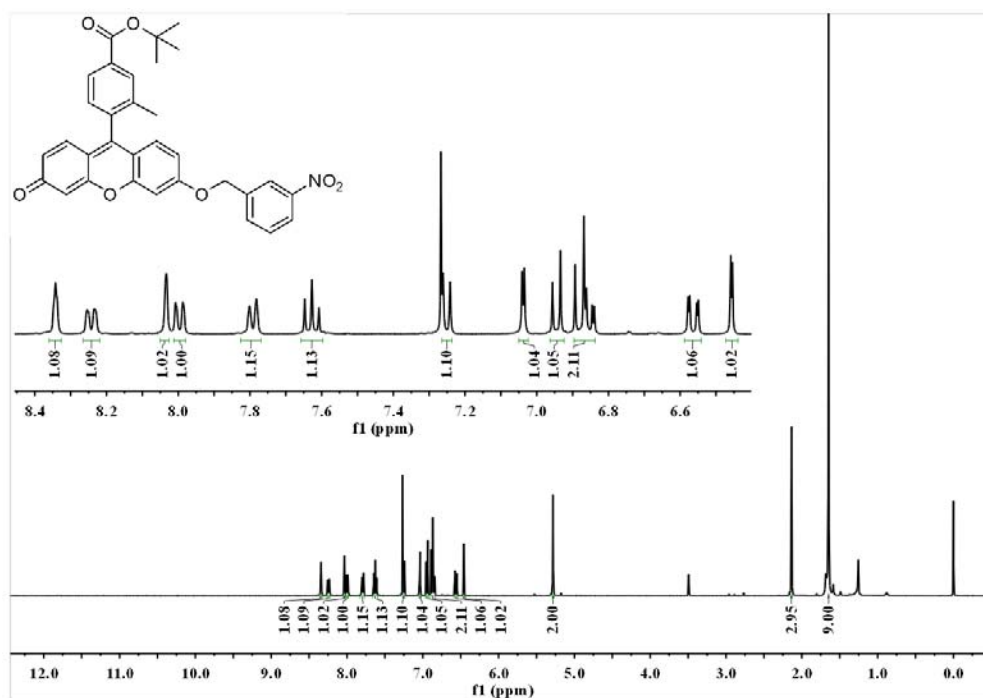


Figure S19. ¹H NMR spectrum of compound 3.

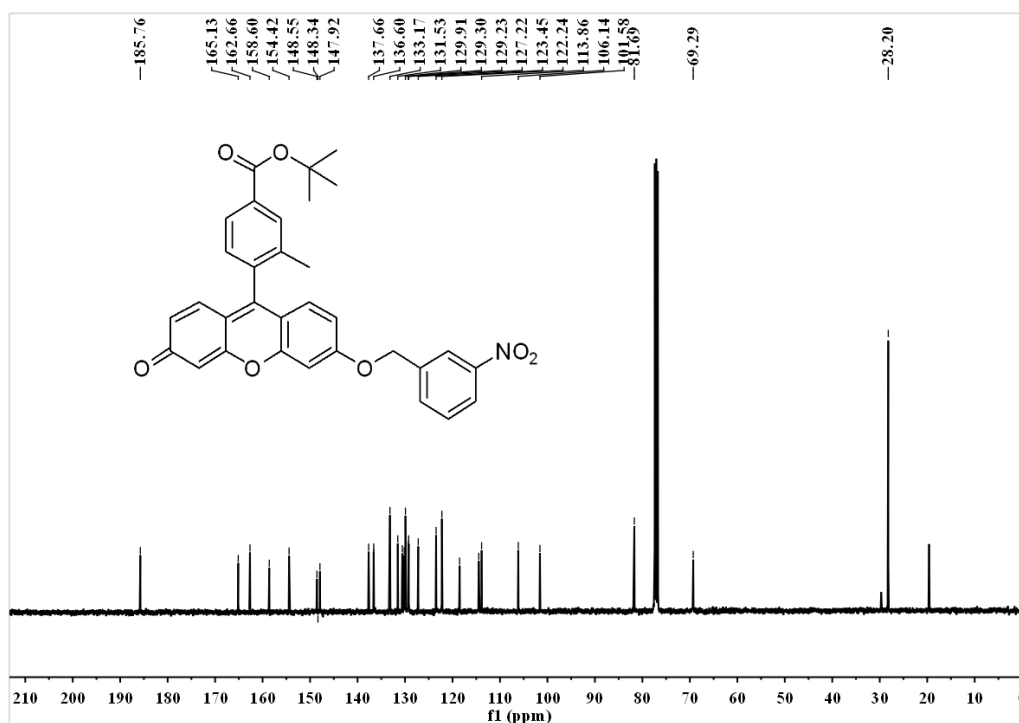


Figure S20. ¹³C NMR spectrum of compound 3.

Elemental Composition Report

Single Mass Analysis

Tolerance = 50.0 PPM / DBE: min = -1.5, max = 100.0

Element prediction: Off

Number of isotope peaks used for i-FIT = 3

Monoisotopic Mass, Even Electron Ions

183 formula(e) evaluated with 12 results within limits (up to 1 closest results for each mass)

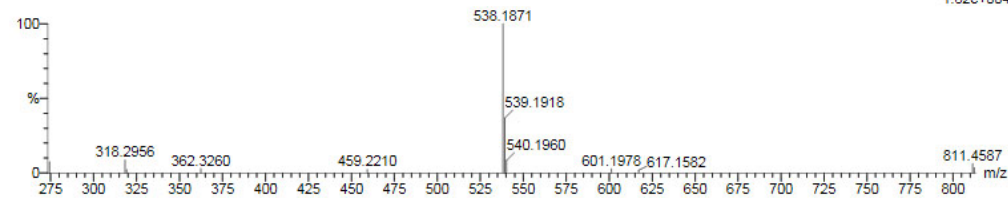
Elements Used:

C: 0-49 H: 0-49 N: 0-3 O: 0-10

JC-WU

ECUST Institute of Fine Chem

JC-LSZ-313 42 (0.361) Cm (40.49)



Minimum:

Maximum:

300.0 50.0 -1.5

100.0

Mass

Calc. Mass

mDa

PPM

DBE

i-FIT

i-FIT (Norm)

Formula

538.1871

538.1866

0.5

0.9

19.5

10.2

0.0

C32 H28 N O7

Figure S21. Mass spectrum of compound 3.

Compound 4:

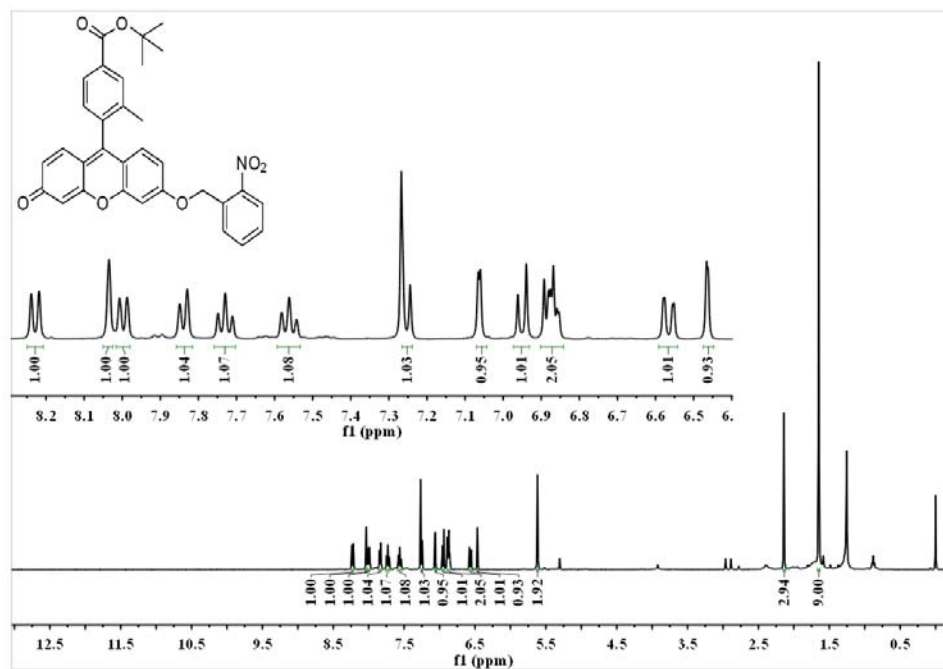


Figure S22. ^1H NMR spectrum of compound 4.

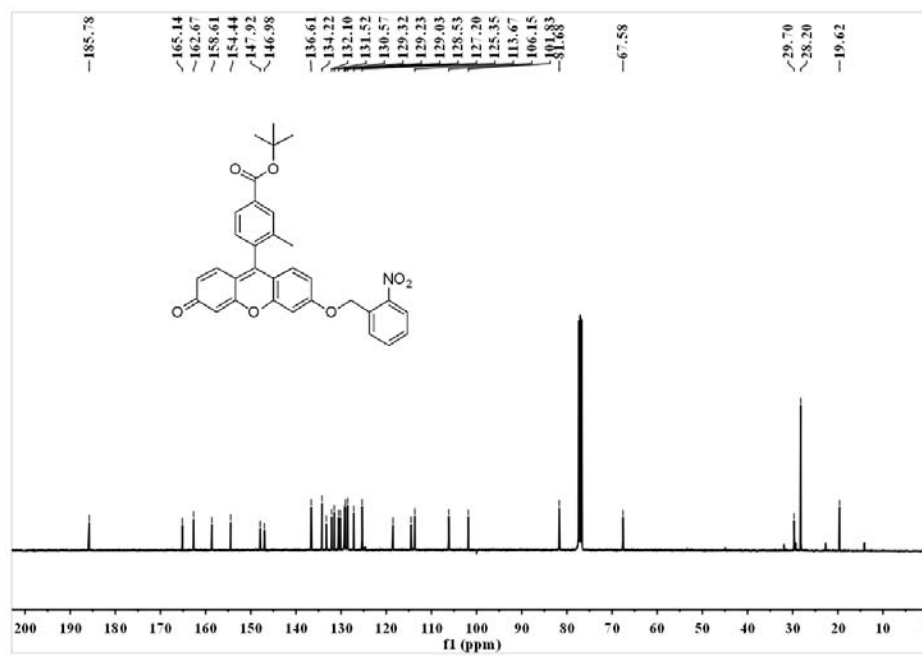


Figure S23. ^{13}C NMR spectrum of compound 4.

Elemental Composition Report

Single Mass Analysis

Tolerance = 50.0 PPM / DBE: min = -1.5, max = 100.0

Element prediction: Off

Number of isotope peaks used for i-FIT = 3

Monoisotopic Mass, Even Electron Ions

13 formula(e) evaluated with 1 results within limits (up to 1 closest results for each mass)

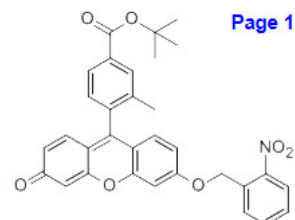
Elements Used:

C: 0-32 H: 0-49 N: 0-1 O: 0-7

JC-WU

ECUST institute of Fine Chem

JC-LSZ-315 2 (0.117) Cm (2:12)



Page 1

02-Jun-2016

19:50:12

1: TOF MS ES+

1.49e+004

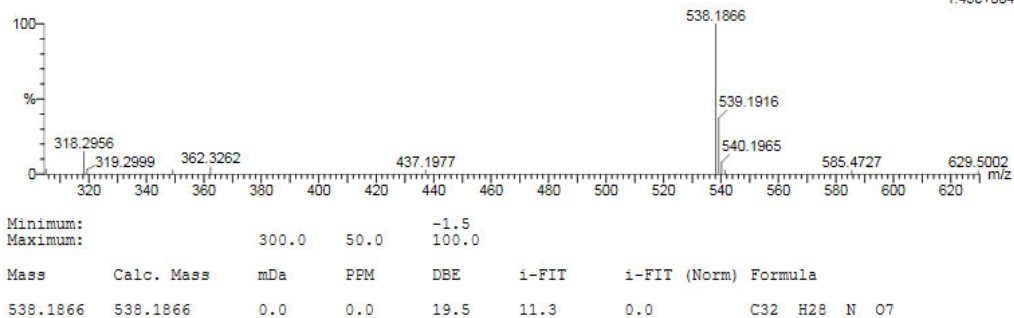


Figure S24. Mass spectrum of compound 4.

FBN-1:

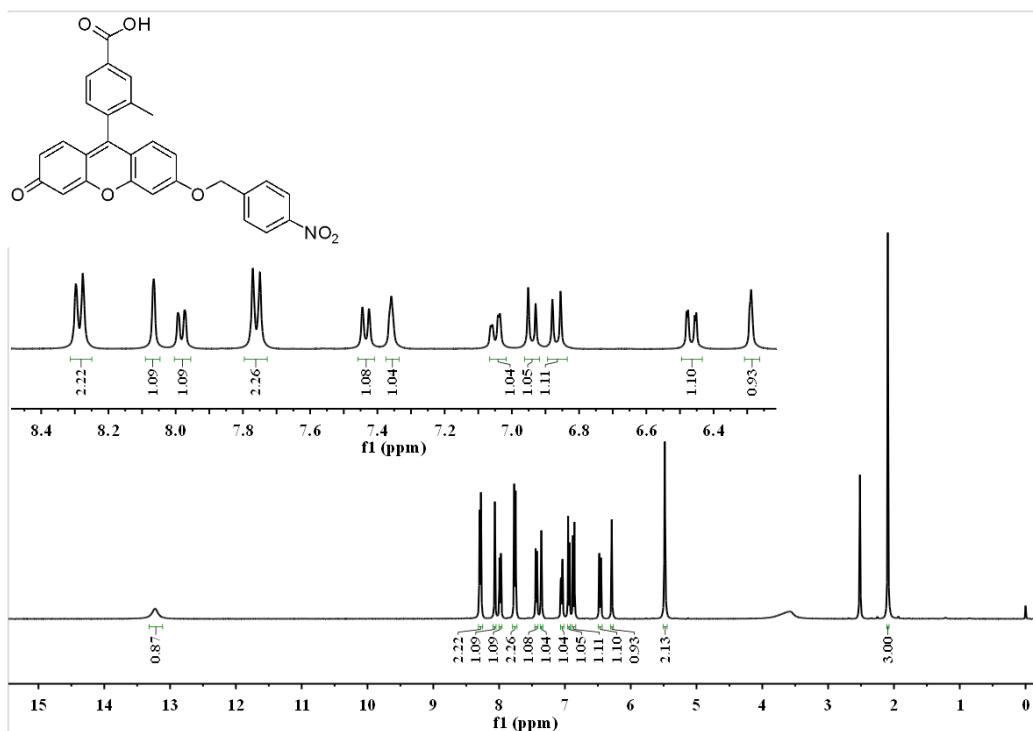


Figure S25. ¹H NMR spectrum of FBN-1.

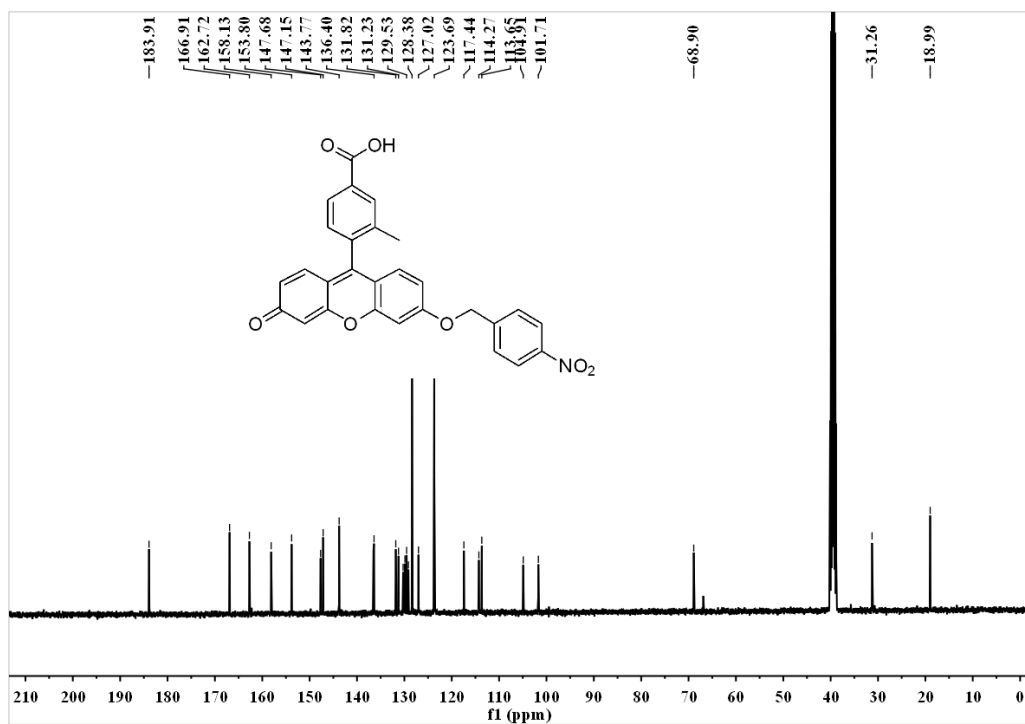


Figure S26. ¹³C NMR spectrum of FBN-1.

Elemental Composition Report

Single Mass Analysis

Tolerance = 50.0 PPM / DBE: min = -1.5, max = 100.0

Element prediction: Off

Number of isotope peaks used for i-FIT = 3

Monoisotopic Mass, Even Electron Ions

23 formula(e) evaluated with 1 results within limits (up to 1 closest results for each mass)

Elements Used:

C: 0-28 H: 0-100 N: 0-1 O: 1-7

JC-WU

ECUST Institute of Fine Chem

JC-LSZ-107 46 (0.370) Cm (45.48)

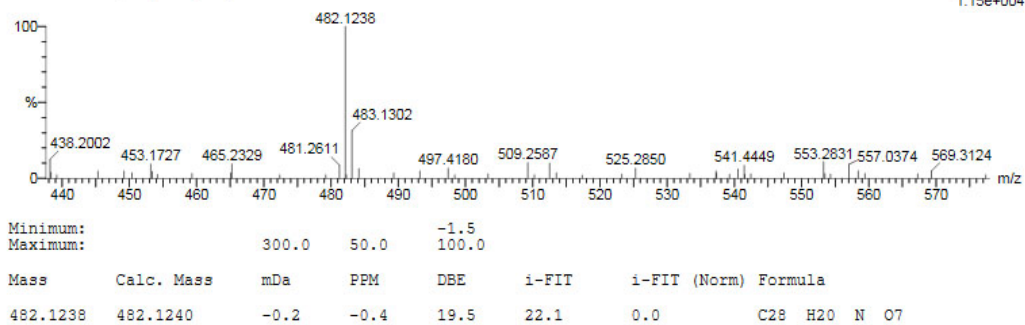
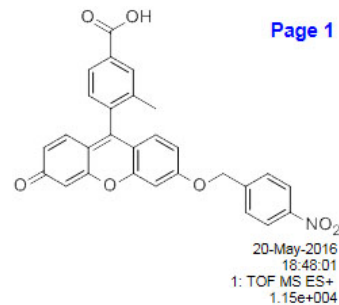


Figure S27. Mass spectrum of the FBN-1.

FBN-2:

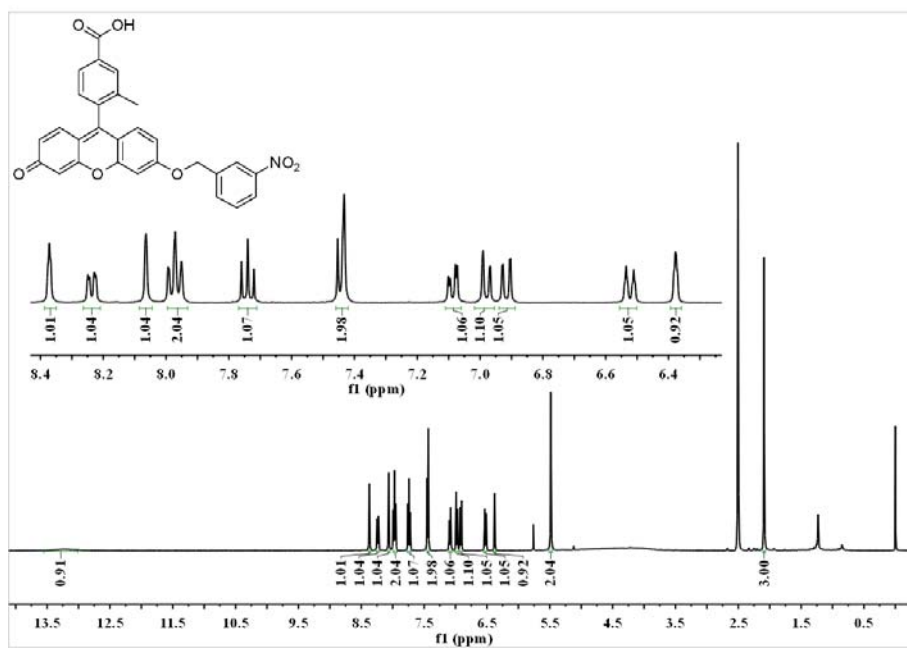


Figure S28. ¹H NMR spectrum of FBN-2.

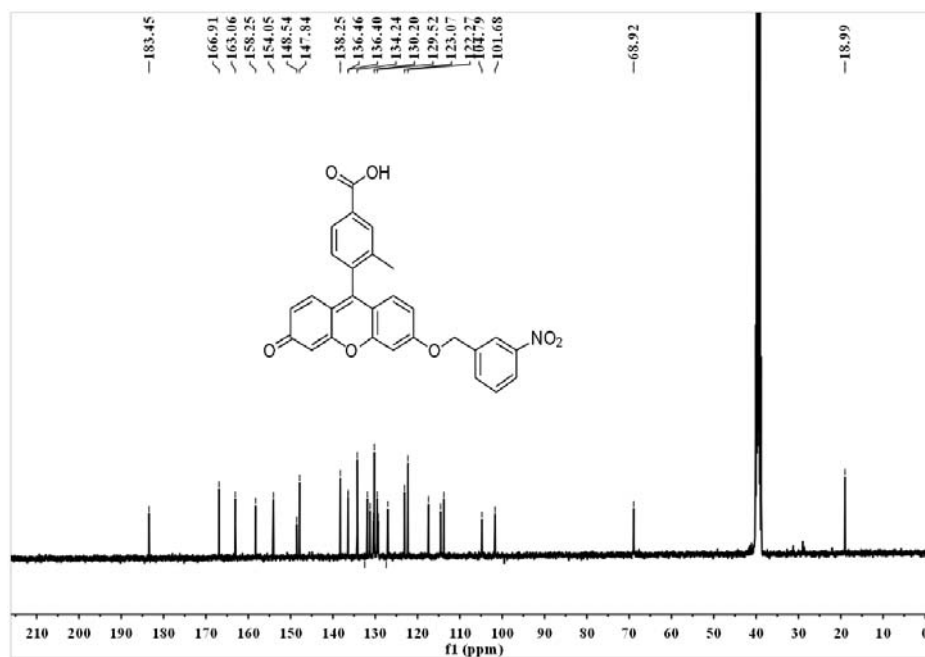


Figure S29. ¹³C NMR spectrum of FBN-2.

Elemental Composition Report

Page 1

Single Mass Analysis

Tolerance = 50.0 PPM / DBE: min = -1.5, max = 100.0

Element prediction: Off

Number of isotope peaks used for i-FIT = 3

Monoisotopic Mass, Even Electron Ions

183 formula(e) evaluated with 10 results within limits (up to 1 closest results for each mass)

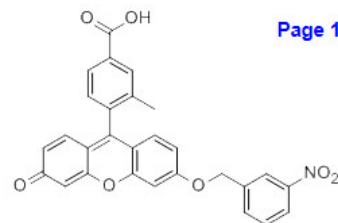
Elements Used:

C: 0-49 H: 0-49 N: 0-3 O: 0-10

JC-WU

ECUST Institute of Fine Chem

JC-LSZ-314 86 (0.624) Cm (81:87)



02-Jun-2016
20:06:35
1: TOF MS ES+
2.50e+003

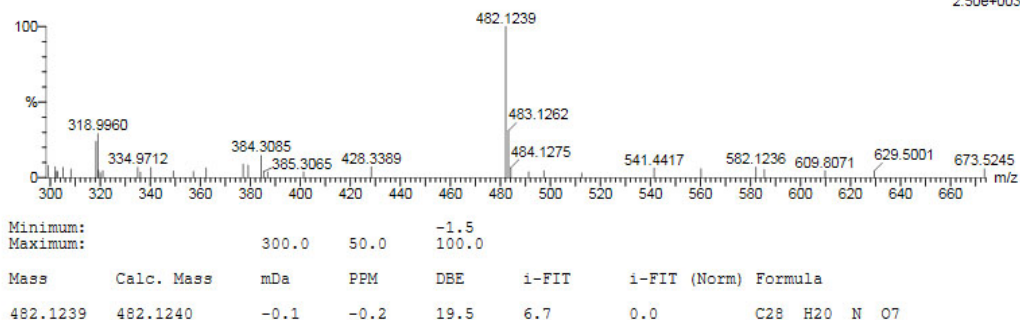


Figure S30. Mass spectrum of the FBN-2.

FBN-3:

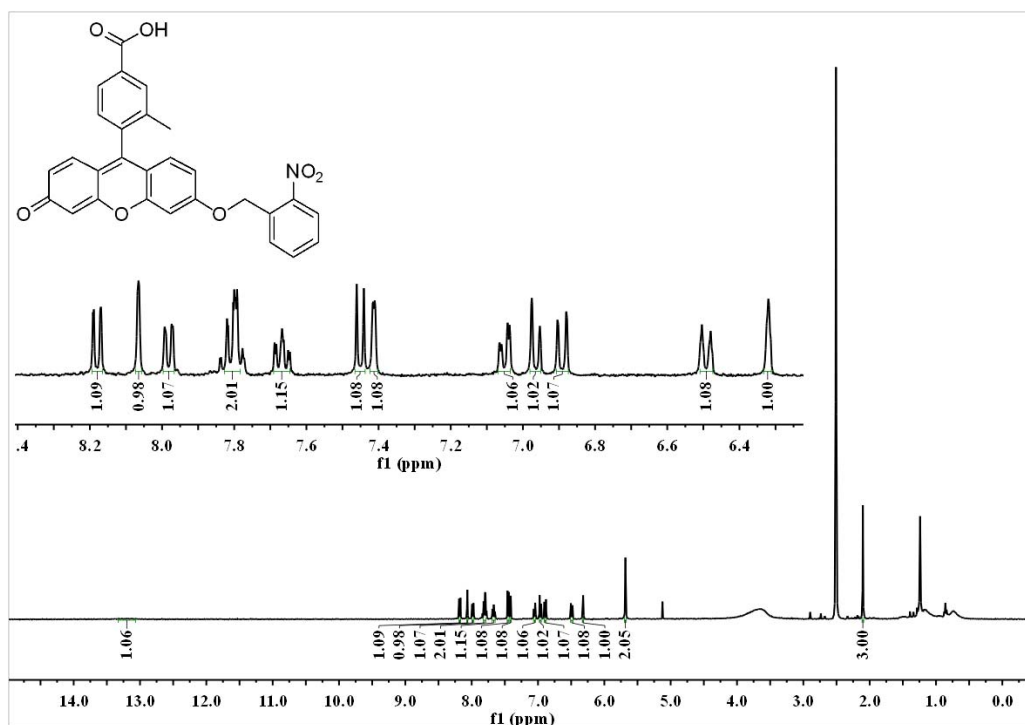


Figure S31. ¹H NMR spectrum of FBN-3.

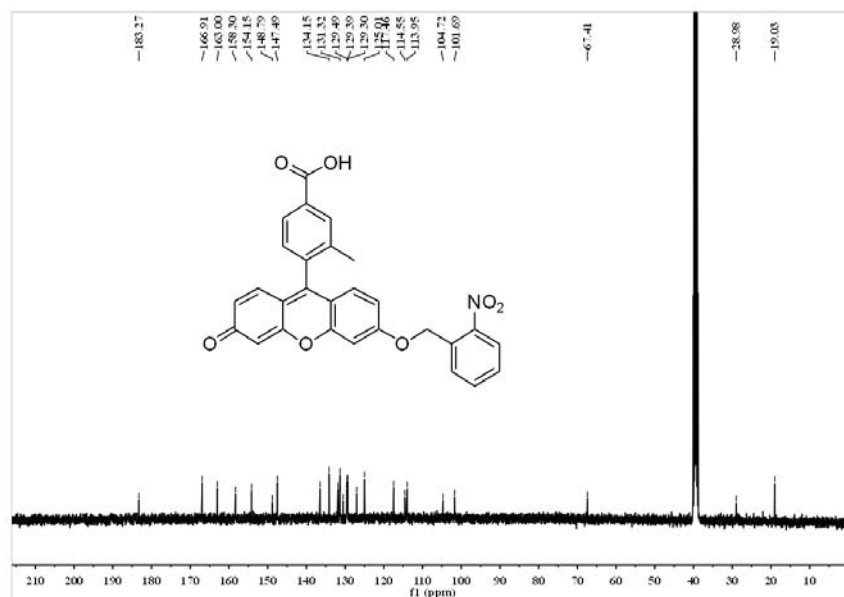


Figure S32. ^{13}C NMR spectrum of FBN-3.

Elemental Composition Report

Single Mass Analysis

Tolerance = 50.0 PPM / DBE: min = -1.5, max = 100.0

Tolerance = 50.0 FPM
Element prediction: Off

Number of isotope peaks used for i-FIT = 3

Monoisotopic Mass, Even Electron Ions

16 formula(e) evaluated with 1 results within limits (up to 1 closest results for each mass)

Elements Used:

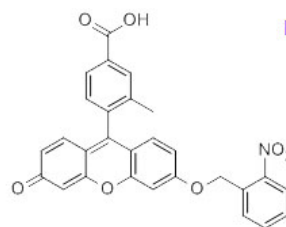
C: 0-28 H: 0-49 N: 0-1 O: 0-7

JC-WU

ECUST institute of Fine Chem

JC-LSZ-316 19 (0.205) Cm (19:46)

Page 1



02-Jun-2016

19:44:54

1: TOF MS ES+

2.18e+004

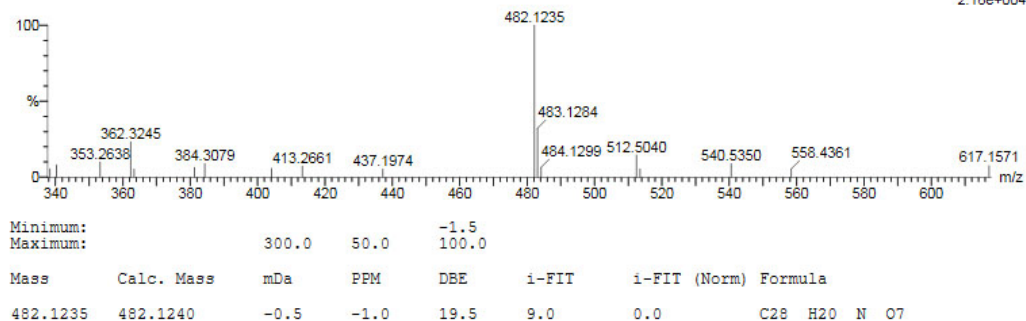


Figure S33. Mass spectrum of the FBN-3.

References

- (1) Rammler, D. H. The effect of dmso on several enzyme systems. *Ann. N. Y. Acad. Sci.*, **1967**, 141(1), 291–299.
- (2) Wood, D. C.; Wood, J. Pharmacologic and biochemical considerations of dimethyl sulfoxide. *Ann. N. Y. Acad. Sci.*, **1975**, 243(1), 7–19.
- (3) Zaks, A.; Klibanov, A. M. Enzyme-catalyzed processes in organic solvents. *Proc. Natl. Acad. Sci.*, **1985**, 82, 3192–3196.
- (4) Feng, P.; Zhang, H.; Deng, Q.; Liu, W.; Yang, L.; Li, G.; Chen, G.; Du, L.; Ke, B.; Li, M. Real-time bioluminescence imaging of nitroreductase in mouse model. *Anal. Chem.* **2016**, 88, 5610–5614.
- (5) Li, Y.; Sun, Y.; Li, J.; Su, Q.; Yuan, W.; Dai, Y.; Han, C.; Wang, Q.; Feng, W.; Li, F. Y. Ultrasensitive near-infrared fluorescence-enhanced probe for in vivo nitroreductase imaging. *J. Am. Chem. Soc.* **2015**, 137, 6407–6416.
- (6) Zhang, J.; Liu, H.; Hu, X.; Li, J.; Liang, L.; Zhang, X.; Tan, W. H. Efficient two-photon fluorescent probe for nitroreductase detection and hypoxia imaging in tumor cells and tissues. *Anal. Chem.* **2015**, 87, 11832–11839.
- (7) Guo, T.; Cui, L.; Shen, J.; Zhu, W.; Xu, Y.; Qian, X. A. Highly sensitive long-wavelength fluorescence probe for nitroreductase and hypoxia: selective detection and quantification. *Chem. Commun.* **2013**, 49, 10820–10822.
- (8) Xu, K.; Wang, F.; Pan, X.; Liu, R.; Ma, J.; Kong, F.; Tang, B. High selectivity imaging of nitroreductase using a near-infrared fluorescence probe in hypoxic tumor. *Chem. Commun.* **2013**, 49, 2554–2556.
- (9) Okuda, K.; Okabe, Y.; Kadonosono, T.; Ueno, T.; Youssif, B. G. M.; Kizaka-Kondoh, S.; Nagasawa, H. 2-Nitroimidazole-tricarbocyanine conjugate as a near-infrared fluorescent probe for in vivo imaging of tumor hypoxia. *Bioconjugate Chem.* **2012**, 23, 324–329.